Watenphul, A., Wunder, B., Heinrich, W. (2009): High-pressure ammonium-bearing silicates: Implications for nitrogen and hydrogen storage in the Earth's mantle. - American Mineralogist, 94, 2-3, 283-292

DOI: 10.2138/am.2009.2995

High-pressure ammonium-bearing silicates: implications for nitrogen and hydrogen storage in the Earth's mantle

Anke Watenphul*, Bernd Wunder, and Wilhelm Heinrich

Deutsches GeoForschungsZentrum (GFZ), Telegrafenberg, 14473 Potsdam, Germany, Section 4.1 * E-mail: watenphul@gfz-potsdam.de

Abstract

The ammonium analogues of the high-pressure potassium-bearing silicate phases K-hollandite, K-Si-wadeite, K-cymrite, and phengite were synthesized in the system $(NH_4)_2O(-MgO) - Al_2O_3 - SiO_2 - H_2O$ (N(M)ASH) using multi-anvil and piston-cylinder equipment. Syntheses included NH_4-hollandite $[NH_4AlSi_3O_8]$ at 12.3 GPa, 700 °C; NH_4-Si-wadeite $[(NH_4)_2Si_4O_9]$ at 10 GPa, 700 °C; NH_4-cymrite $[NH_4AlSi_3O_8 \cdot H_2O]$ at 7.8 GPa, 800 °C; and NH_4-phengite $[NH_4(Mg_{0.5}Al_{1.5})(Al_{0.5}Si_{3.5})O_{10}(OH)_2]$ at 4 GPa, 700 °C. Run products were characterized by SEM, FTIR, and powder XRD with Rietveld refinements. Cell parameters of the new NH_4 end-members were determined to $a = 9.4234(9)$ Å, $c = 2.7244(3)$ Å, $V = 241.93(5)$ Å^3 (NH_4-hollandite); $a = 6.726(1)$ Å, $c = 9.502(3)$ Å, $V = 372.3(1)$ Å^3 (NH_4-Si-wadeite); $a = 5.3595(3)$ Å, $c = 7.835(1)$ Å, $V = 194.93(5)$ Å^3 (NH_4-cymrite). NH_4-phengite consisted of a mixture of $1M, 2M_1, 2M_2, 3T$, and $2Or$ polytypes. The most abundant polytype $2M_1$ has the cell dimensions $a = 5.2195(9)$ Å, $b = 9.049(3)$ Å, $c = 20.414(8)$ Å, $\beta = 95.65(3)°$, $V = 959.5(5)$ Å^3. All unit cell volumes are enlarged in comparison to the potassium analogues. Substitution of NH_4 for K does not cause changes in space group symmetry. NH_4 incorporation was confirmed by the appearance of NH_4 vibration modes ν_4 and ν_3 occurring in the ranges of 1397–1459 and 3223–3333 cm^{-1}, respectively.

Ammonium in eclogite facies metasediments is mainly bound in micas and concentrations may reach up to a few thousand ppm. It can be stored to greater depths in high-pressure potassium silicates during ongoing subduction. This possibly provides an important mechanism for nitrogen and hydrogen transport into the deeper mantle.

Keywords: Hollandite, wadeite, cymrite, phengite, ammonium, high-pressure synthesis, nitrogen cycle

Introduction

There is general agreement that nitrogen has been discharging for a long time from the Earth's mantle to the atmosphere through volcanic and hydrothermal activities (e.g., Javoy et al. 1986; Marty 1995; Sano et al. 2001). It is, however, controversially debated if a substantial amount of nitrogen is recycled during subduction processes. The discussion carried out in a series of recent papers mainly relies on the interpretation of the amount of molecular nitrogen and nitrogen isotope ratios measured in diamonds, mantle xenoliths, basalts, volcanic gases, hydrothermal fluids and the atmosphere, and on the question whether different nitrogen reservoirs in the mantle existed that may have been produced by input of isotopically different nitrogen from subducted sediments (e.g., Mohapatra and Murty 2000; Pinti et al. 2001; Fischer et al. 2002; Busigny et al. 2003; Cartigny and Ader 2003; Marty and Dauphas 2003a, 2003b; Mather et al. 2004; Fischer et al. 2005; Pitcairn et al. 2005; Thomassot et al. 2007).

Nitrogen in sediments has an organic origin. Under anoxic conditions at about 150 °C amino acids decompose to NH_4, which is incorporated into clay minerals, micas and feldspars substituting for K in small but significant amounts (Williams et al. 1992). It has been shown that during progressive contact and Barrovian-type metamorphism NH_4 is continuously released so that in high-grade rocks less than 10 % of the original nitrogen remains (Bebout and Fogel 1992; Bebout et al. 1999; Sadofsky and Bebout 2000; Mingram and Bräuer 2001; Pöter et al. 2004; Pitcairn et al. 2005). By contrast, Busigny et al. (2003) showed that in high-pressure low-temperature metapelites and metabasites from the Western Alps the entire nitrogen, up to 1600 ppm mainly bound as NH_4 in micas, remains in the rock up to at least 3 GPa. It would appear that there is no information about the fate of nitrogen in subducting slabs beyond that, and we do not know if and how nitrogen could be transported into the deeper mantle.

NH_4^+ has an ionic radius similar to Rb^+ (Shannon 1976) and replaces K^+ in silicates. One may reasonably assume that under slab conditions NH_4 persists in rocks as long as K-feldspar and high-pressure micas remain stable. In a status report on the stability of K-phases at mantle conditions, Harlow and Davies (2004) documented a number of K-bearing silicates that may form at higher pressure, mainly based on a summary of experimental results. In a wet system, K-feldspar may be replaced by K-cymrite [$K^{IV}Al^{IV}Si_3O_8 \cdot H_2O$] above about 2.5 GPa (Fasshauer et al. 1997; Fig. 1). K-cymrite is stable up to about 9 GPa, where it decomposes to K-hollandite [$K^{VI}Al^{Vl}Si_3O_8$] and fluid (Thompson et al. 1998). In a dry system, K-feldspar reacts to K-Si-wadeite [$K_2^{VI}Si^{IV}Si_3O_9$], (also termed Si-wadeite; Harlow and Davies 2004; Yong et al. 2008) + kyanite + coesite above 5 to 6.5 GPa, 400 to 1000 °C (Yagi et al. 1994; Urakawa et al. 1994). At pressures higher than about 9 GPa, the stability of K-Si-wadeite is limited by reactions that typically produce K-hollandite (Yong et al. 2008; Fig. 1). K-hollandite appears also as a reaction product of phengite breakdown in metapelitic and metabasaltic bulk compositions at pressures higher than 8 to 11 GPa, 750 to 900 °C (Domanik and Holloway 1996; Schmidt and Poli 1998; Poli and Schmidt 2002) and is probably stable up to 95 GPa, 2300 °C (Konzett and Fei 2000; Tutti et al. 2001). Therefore, K-hollandite is believed to be the main K-rich solid-phase reservoir for potassium through the transition zone to the lower mantle in silicate compositional systems because K-Al-bearing silicates react to yield K-hollandite with increasing pressure (Harlow

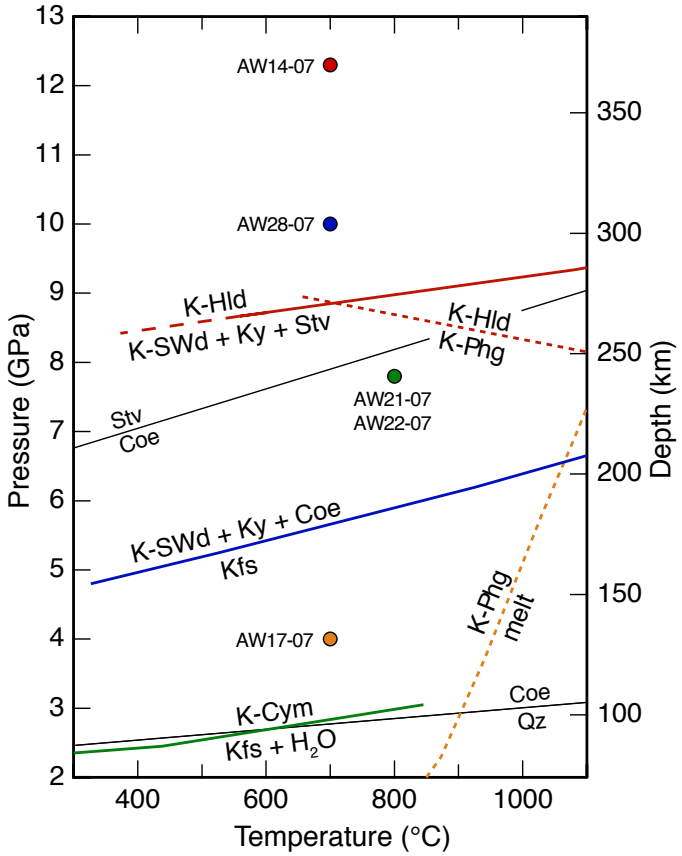

Figure 1: *P–T* plot showing stabilities of relevant high-pressure phases in the $K_2O - (MgO) - Al_2O_3 - SiO_2 - H_2O$ system. Data for K-cymrite from Fasshauer et al. (1997), for K-Si-wadeite and K-hollandite from Yong et al. (2008). Upper temperature and pressure stabilities of K-phengite determined for natural samples of metapelitic bulk compositions (Poli and Schmidt 2002), stabilities of SiO_2 polymorphs from Akaogi et al. (1995). Dots depict synthesis conditions of the NH_4-bearing analogues (Table 1). Abbreviations as in Table 1.

and Davies 2004, and references therein).

All high-pressure K-silicates constitute potential carriers of nitrogen and hydrogen into the deep mantle. The aim of this study is to show that the ammonium end-member analogues of hollandite [$NH_4AlSi_3O_8$], wadeite [$(NH_4)_2Si_4O_9$], cymrite [$NH_4AlSi_3O_8 \cdot H_2O$], and phengite [$NH_4(Mg_{0.5}Al_{1.5})(Al_{0.5}Si_{3.5})O_{10}(OH)_2$] can be synthesized stably at high pressure. Some of their crystal chemical properties are given, along with some speculations on possible transport of nitrogen and hydrogen to greater depths of the Earth.

Experimental and analytical techniques

Experimental procedures

There are some inherent difficulties in synthesizing NH_4-bearing minerals at high pressure. Experiments performed in multi-anvil modules routinely apply heated gels as starting materials. This is impossible in the case of ammonium because it rapidly evaporates during heating. For the synthesis of NH_4-hollandite, NH_4-Si-wadeite, and NH_4-cymrite we therefore used well-characterized, hydrothermally pre-synthesized buddingtonite, [$NH_4AlSi_3O_8$], the NH_4-analogue of sanidine (Harlov et al. 2001a; Pöter et al. 2007) as starting solid. As stabilizing NH_4-phases requires some NH_3/NH_4^+-gas pressure we mainly used a wet system for runs by adding an NH_4OH solution in excess, only run AW22-07 used nominally dry buddingtonite as starting material, but a small amount of water absorption on the sample surface could not be avoided during sample preparation. This produces the required partial pressure of ammonia and keeps the hydrogen fugacity sufficiently high, i.e., the redox conditions reducing, at least as long as the H–N–O fluid provides sufficient hydrogen at given P and T. However, with our setup hydrogen loss from the gold or platinum capsules cannot be completely prevented (see below). Hydrogen loss gradually shifts conditions towards more oxidizing. Molecular nitrogen, N_2, is increasingly produced, finally resulting in the complete decomposition of the ammonium-bearing phase. This behavior was demonstrated by the sliding reaction buddingtonite [$NH_4AlSi_3O_8$] + O_2 → Al_2SiO_5 + SiO_2 + N_2 + H_2O performed in long-run hydrothermal experiments (Harlov et al. 2001a). Run durations were therefore adapted to minimize overall hydrogen loss. For calculation of neutral fluid species and relevant equilibria in the H–N–O system at very high pressure see, e.g., Churakov and Gottschalk (2003a, b). Similarly, NH_4-phengite was synthesized from a SiO_2, γ-Al_2O_3 and MgO oxide mix with NH_4OH solution in excess. Proportions of oxides were according to a phengite composition of [$(NH_4)(Mg_{0.6}Al_{1.4})(Al_{0.4}Si_{3.6})O_{10}(OH)_2$]. The intended celadonite-component chosen here is about that determined by Melzer and Wunder (2000) for (K,Rb,Cs)-bearing phengites synthesized at identical P,T conditions. Solids and fluids were cold-welded either into Pt-capsules (run AW14-07; Table 1) or Au-capsules (runs AW28-07, AW21-07, AW22-07; Table 1) of 3 mm length, 2 mm outer diameter, and 0.2 mm wall thickness. In all but one experiment, a 25% NH_4OH-solution was given in excess to the solid starting material (Table 1). The exact amount of ammonium loaded into the capsules was unknown because of rapid evaporation of a small fraction of ammonia during welding.

Synthesis of NH_4-bearing phengite was performed in a piston-cylinder press. The high-pressure cell consisted of a steel furnace with rock salt and fired pyrophyllite as pressure media. Two Au-capsules of 10 mm length and 3 mm diameter were filled with about 16 mg of solid and fluid starting material and sealed using a plasma arc welder while partly immersed in an ice/water mixture. Pressure was calibrated according to the quartz–coesite transition. For this assembly, the estimated pressure uncertainty is approximately 1%. The temperature was monitored using a chromel-alumel thermocouple; the precision is around ± 2 °C. A detailed description of the press and the experimental method is given in Wunder (1998).

After the experiments the capsules were carefully separated from the assembly material. They were cleaned in an ultrasonic bath for 10 min in ethanol and carefully opened. To exclude that the measured ammonium in the different analytical methods was due to outside

Table 1. Starting material, experimental conditions and run products

Run no.	Starting material	P (GPa)	T (°C)	t (h)	Run products (wt%)
AW14-07	Buddingtonite + NH_4OH solution	12.3	700	6	NH_4-Hld (31), Stv (22), NH_4-SWd (17), OH-Top (8), Ky (21), Egg (< 1)
AW28-07	Buddingtonite + NH_4OH solution	10.0	700	24	NH_4-SWd (34), OH-Top (39), Stv (27)
AW21-07	Buddingtonite + NH_4OH solution	7.8	800	24	NH_4-Cym (70), Coe (23), Ky (7)
AW22-07	Buddingtonite (nominally dry)	7.8	800	24	NH_4-Cym (49), Coe (26), Ky (25)
AW17-07	Oxide mixture + NH_4OH solution	4.0	700	26	NH_4-Phg $2M_1$ (75), NH_4-Phg $3T$ (14), NH_4-Phg $2Or$ (4), NH_4-Phg $1M$ (< 1), NH_4-Phg $2M_2$ (< 1), Coe (6), Ky (tr)*

* Traces of kyanite only detected by EMP.
Abbreviations: Coe: coesite, Ky: kyanite, NH_4-Cym: NH_4-cymrite, NH_4-Hld: NH_4-hollandite, NH_4-Phg: NH_4-phengite, NH_4-SWd: NH_4-Si-wadeite, OH-Top: OH-topaz, Stv: stishovite, Egg: Phase Egg.
Amount of run products (wt%) calculated from Rietveld refinements.

NH_4-hollandite, NH_4-Si-wadeite and NH_4-cymrite were synthesized using a rotating multi-anvil apparatus (Table 1). The advantage of rocking or rotating versus static systems for fluid-bearing charges is outlined in Schmidt and Ulmer (2004). To prevent separation of fluid and solid components, experiments were performed by 360°-rotation of the Walker-type module with a speed of 4°/s. The tungsten carbide anvils had a truncation edge length of 8 mm. Sample assemblies (Fig. 2) consisted of an MgO (+ 5% Cr_2O_3) octahedra with an edge length of 14 mm. The inner parts of the assembly were made up of a zirconia oxide sleeve, a stepped graphite heater, a Mo-disk and ring, and an axial thermocouple with wires of different W–Re alloys. Hexagonal boron nitride around the capsules was used as inner pressure medium because it was shown to behave relatively impermeable to hydrogen in piston cylinder experiments (Truckenbrodt et al. 1997), so that the furnace would not control the hydrogen fugacity of the sample within a reasonable time-span. The temperature was measured using a W5%Re–W26%Re (Type C) thermocouple. To protect the thermocouple wires, we used coils of the same material as the wires to eliminate any influences on the EMF of the thermocouples (Nishihara et al. 2006). The precision of the thermocouple is about ± 10 °C. The pressure calibration was performed by press-load experiments based on room temperature phase transitions in Bi and high-temperature phase transitions (quartz–coesite; $CaGeO_3$ garnet–perovskite; coesite–stishovite; forsterite–wadsleyite). The precision along the pressure range of this study is approximately ± 0.2 GPa.

contamination of the crystals, the run products were washed with 50 ml warm bi-distilled water and afterwards dried at 100 °C for several days.

Analytical methods

Powder X-ray diffraction (XRD). The run products were ground for several minutes in an agate mortar, diluted with Elmer's White glue and spread evenly on a "zero scattering" circular foil. Preferential orientation of the crystals was minimized by constantly stirring the sample during the drying process. The sample was covered with an empty foil and mounted

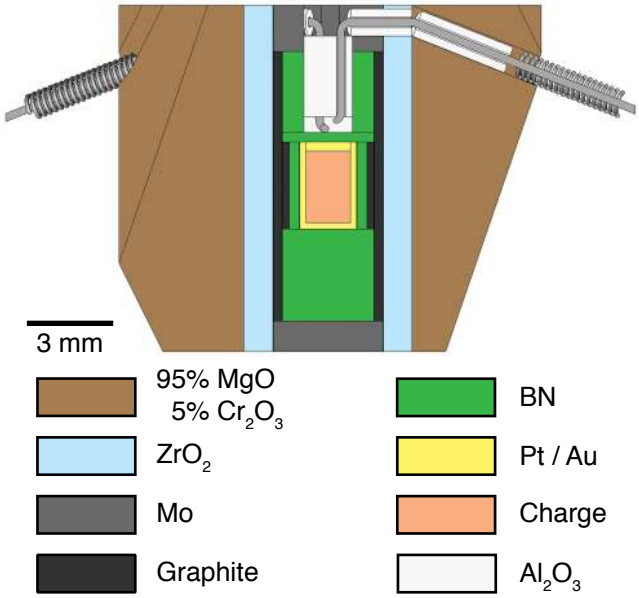

Figure 2: Schematic cross section of the 14/8 mm assembly used for multi-anvil experiments.

into a transmission sample holder. Powder XRD-patterns were recorded in transmission with a fully automated STOE STADI P diffractometer using CuKα_1-radiation at 40 kV and 40 mA, a take-off angle of 6°, a primary monochromator, and a 7° wide position-sensitive detector (PSD). The intensities were recorded between 5° and 125° 2θ with a detector step size of 0.1° and a resolution of 0.02°. Counting times were selected to result in a maximum intensity of around 3000 counts; this was due to about 20 s per detector step. The collected patterns were processed using the GSAS software package for Rietveld refinement (Larson and von Dreele 2004) for phase identification, phase proportions, and unit cell parameters. The refinement procedure for NH_4-bearing phases followed that of Pöter et al. (2007). Initial crystal structures were taken from the Inorganic Crystal Structure Database (ICSD, FIZ Karlsruhe, http://icsdweb.FIZ-karlsruhe.de). For input parameters, the structures of the respective potassium end-members were modified in that K was replaced by Na, because Na has the same number of electrons as NH_4. Due to the complexity of the NH_4-phengite sample (AW17-07, Table 1) with five polytypes ($1M, 2M_1, 2M_2, 3T$ and $2Or$), and coesite and kyanite as additional phases, the refinement was kept as simple as possible, i.e., common profile parameters were used for all mica polytypes by setting appropriate constraints. The statistical parameters χ^2 and Durbin-Watson (DW) of Rietveld refinements from all runs are within the ranges of $1 < \chi^2 < 1.26$ and $1.23 < \mathrm{DW} < 1.48$.

Infrared (IR) spectroscopy. About 1 mg of the run products was ground in an agate mortar and then mixed with 450 mg of dried KBr. The homogenized mixture was subsequently pressed into 13 mm diameter transparent pellets under vacuum and then dried for several days at 170 °C. Measurements were carried out in the spectral range from 4000 cm^{-1} to 400 cm^{-1} with a resolution of 2 cm^{-1} using a Bruker IFS 66vFTIR spectrometer equipped

with a globar as light source, a KBr beam-splitter and a DTGS-detector. The sample chamber of the interferometer was evacuated down to 200 Pa so that the influence of atmospheric H_2O and CO_2 was negligible. The measured spectra were averaged over 256 scans. The interferograms were phase-corrected after the procedure of Mertz (1965) and Griffiths and de Haseth (1986). Blackman-Harris 3-term mode was chosen as apodization function. The measured spectra were transformed into transmission spectra. After background correction the band center, FWHM, and integral intensity of each band were determined using the program PeakFit by Jandel Scientific.

Electron microprobe (EMP) analyses. Polished grain mounts of NH_4-hollandite from run AW14-07 and NH_4-phengite from run AW17-07 were measured using a JEOL JXA-8500F field emission electron probe microanalyzer in the wavelength-dispersive mode (WDS). As standards orthoclase (Al), wollastonite (Si) and periclase (Mg), only for the NH_4-phengites, were used. Attempts to obtain "good" nitrogen concentrations were not successful because crystal sizes are too small, count yields are low and NH_4-phases tend to decompose under the beam at long counting rates. Operating conditions were 10 kV, 5 nA and a beam diameter of about 50 nm. On-peak counting times were 10 s for Si and Al and 20 s for Mg. Background on both sides of the peak was measured for 5 and 10 s, respectively. Conditions were chosen carefully to reduce the damage of the mica under the electron beam. NH_4-hollandite crystals did not exceed 1 μm in width and 800 nm in thickness, NH_4-phengite crystals 2 μm in width and 250 nm in thickness. Calculation of the penetration depth of the focused electron beam resulted in about 1200 nm. Analyses of the NH_4-hollandite crystals were accepted, if the oxide sum, i.e., $SiO_2 + Al_2O_3$ was between 88.6 and 92.2 wt%; 89.9 wt% would represent an ideal NH_4-hollandite having 1 $(NH_4)_2O$ pfu. In case of the NH_4-phengites analyses were accepted, if $SiO_2 + MgO + Al_2O_3$ was between 84 and 88.3 wt%, the latter representing an ideal NH_4-phengite having additionally 1 $(NH_4)_2O$ and 1 H_2O pfu. The composition of NH_4-hollandite was calculated on the basis of 8 oxygens and assuming full occupation of the interlayer site. The NH_4-phengite composition was calculated on the basis of 11 oxygens assuming ideal dioctahedral micas with 2/3 of the octahedral and all of the tetrahedral sites occupied, full occupation of the interlayer site by one NH_4, and two OH groups pfu. Because nitrogen was not measured, possible deficiencies in interlayer NH_4 and concomitant occurrence of some pyrophyllite or talc component in NH_4-phengite (see Pöter et al. 2007; for synthetic NH_4-muscovite) are disregarded.

Scanning electron microscopy (SEM). Reaction products were characterized using a high resolution Hitachi S-4000 instrument at the TU Berlin. Individual phases (Table 1) were identified by EDS-analysis of the respective elements.

Results

Starting materials, experimental conditions and relative amounts of run products are summarized in Table 1. All experiments produced new NH_4-phases, though always with additional phases in various amounts. Run AW14-07 (12.3 GPa, 700 °C) produced NH_4-hollandite along with NH_4-Si-wadeite, stishovite, OH-topaz, kyanite, and traces of phase Egg. Run AW28-07 (10.0 GPa, 700 °C) yielded NH_4-Si-wadeite together with OH-topaz and stishovite. Run AW21-07 (7.8 GPa, 800 °C) gave NH_4-cymrite plus coesite and kyan-

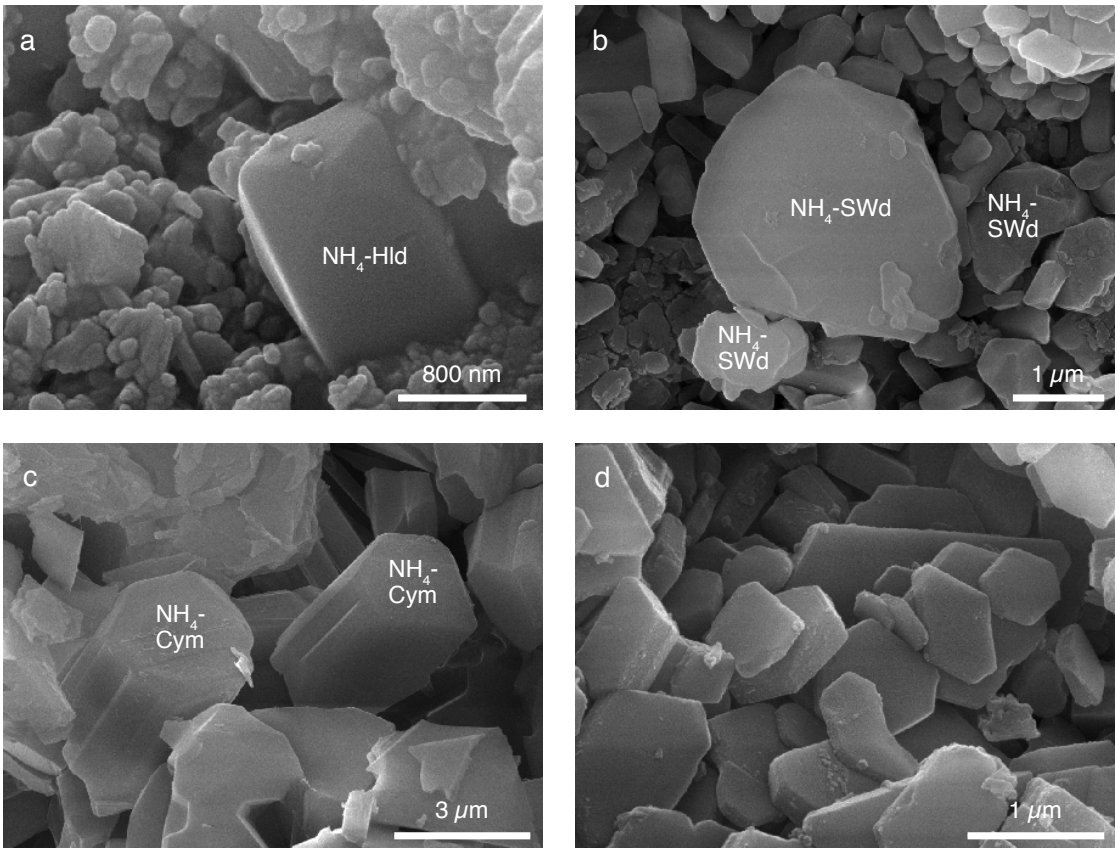

Figure 3: Scanning electron micrographs of the run products. **(a)** NH_4-hollandite, run AW14-07. **(b)** NH_4-Si-wadeite, OH-topaz, and stishovite, run AW28-07. **(c)** NH_4-cymrite, run AW22-07. **(d)** NH_4-phengite, run AW17-07.

ite. Run AW22-07, at initially dry starting conditions and identical P and T of 7.8 GPa, 800 °C also produced NH_4-cymrite plus coesite and kyanite. In AW17-07 (4 GPa, 700°C) various polytypes of NH_4-phengite were produced, along with traces of coesite and kyanite. SEM-micrographs of run products with the relevant phases NH_4-hollandite, NH_4-Si-wadeite, NH_4-cymrite, and NH_4-phengite are shown in Figure 3a-d. Grain sizes of all new NH_4-phases rarely exceed 3 μm. NH_4-hollandite, NH_4-cymrite and NH_4-phengite form idiomorphic crystals with typical tetragonal (NH_4-Hld; Fig. 3a), hexagonal (NH_4-Cym; Fig. 3c) and pseudohexagonal (NH_4-Phg; Fig. 3d) crystal shapes. Glass or any phase resembling quenched melt was not observed in any of the experimental products.

Unit cell dimensions of NH_4-hollandite, NH_4-Si-wadeite and NH_4-cymrite are given in Table 2 along with that of their potassium-bearing analogues. The substitution of NH_4 for K does not induce changes in space group symmetry of the three new NH_4-phases when compared to their respective K-analogues. Lattice parameters, however, change significantly due to the incorporation of the larger NH_4^+ instead of the K^+ cation. The ionic radius of K^+ in VI, VIII, and XII-fold coordination is 1.38, 1.51, and 1.64 Å, respectively (Shannon

Table 2. Lattice parameters of NH_4-bearing high-pressure phases calculated from Rietveld refinements. For comparison, respective K-phases are also given.

Phase	*a* (Å)	*c* (Å)	*V* (Å^3)	Space group
NH_4-hollandite	9.4234(9)	2.7244(3)	241.93(5)	*I4/m*
K-hollandite*	9.315(4)	2.723(4)	236.3(4)	
NH_4-Si-wadeite	6.726(1)	9.502(3)	372.3(1)	*P6$_3$/m*
K-Si-wadeite†	6.6124(9)	9.5102(8)	360.11(7)	
NH_4-cymrite	5.359(1)	7.835(9)	194.93(2)	*P6/mmm*
K-cymrite‡	5.3348(1)	7.7057(1)	189.924(8)	

*Zhang et al. (1993)
† Swanson and Prewitt (1983)
‡ Fasshauer et al. (1997)

1976), whereas that of NH_4^+ is about 1.59, 1.68, and 1.80 Å. The latter values are estimated from composition-volume relationships of alkali-bearing silicates (M. Gottschalk, personal communication).

For NH_4-hollandite, the average of 17 EMP analyses results in $NH_4Al_{1\pm0.03}Si_{3\pm0.03}O_8$, assuming 1 NH_4^+ pfu. The average of 21 EMP analyses for NH_4-phengites results in $NH_4(Mg_{0.45\pm0.03}Al_{1.53\pm0.03})(Al_{0.49\pm0.03}Si_{3.51\pm0.03})O_{10}(OH)_2$, also assuming 1 NH_4^+ pfu. The NH_4-celadonite component of the NH_4-phengites is slightly lower than that given by the NMASH bulk composition. The five polytypes $1M, 2M_1, 2M_2, 3T$ and $2Or$ are present, with $2M_1$ (75%) and $3T$ (14%) as the predominant phases (Table 1). Unit cell parameters of the polytypes are presented in Table 3. They were calculated using the multi-polytype refinement model for synthetic K-phengite polytype mixtures proposed by Schmidt et al. (2001). Polytypes $2Or, 1M$ and $2M_2$ occur in minor or minute amounts and their cell parameters are somewhat less reliable. For comparison, unit cell parameters of synthetic $2M_1$ and $1M$ K-phengites with K-celadonite components similar to our NH_4-celadonite components are also given (Table 3; data for K-phengites from Massonne and Schreyer 1986).

IR spectra of run products AW14-07, AW28-07, AW22-07, and AW17-08 are presented

Table 3. Lattice parameters of NH_4-phengite polytypes produced in run AW17-07. Data calculated from Rietveld refinements.

Phase	*a* (Å)	*b* (Å)	*c* (Å)	β (°)	*V* (Å^3)	Space group
NH_4-Phg *2M$_1$*	5.2204(8)	9.049(2)	20.44(1)	95.71(3)	960.9(5)	*C2/c*
NH_4-Phg *3T*	5.220(2)	30.64(2)			723.2(6)	*P3$_1$12*
NH_4-Phg *2Or*	5.220(2)	8.992(7)		20.65(4)	969(2)	*Pnmn*
NH_4-Phg *1M*	5.315(4)	9.067(4)	10.46(1)	101.79(8)	493.1(7)	*C2*
NH_4-Phg *2M$_2$*	8.93(1)	5.198(5)	20.77(3)	99.3(1)	952(2)	*C2/c*
K-Phg *2M$_1$*	5.2118(6)	9.041(2)	19.972(1)	95.44(6)	936.3(1)	*C2/c*
K-Phg *1M*	5.201(1)	9.026(2)	10.131(4)	101.12(2)	468.5(4)*	*C2/c*

Notes: Data for K-phengite are from Massonne and Schreyer (1986); their experiments V90 (*2M$_1$*) and V270 (*1M*).
*calculated from lattice parameters.

Table 4. Band assignments for vibration modes (ν) with respect to the band centers in cm^{-1} along with relative intensities.

ν	$(NH_4)^+$*	NH_4-Hld	NH_4-SWd	NH_4-Cym	NH_4-Phg	Budd	Tob†
ν_4	1397	1402 sh (m)	1397 sh (m)	1404 sh (w)	1407 sh (m)	1402 sh (w)	1430 (s)
		1436 (s)	1422 (s)	1423 (s)	1433 (s)	1423 sh (m)	1475 sh (m)
		1459 sh (m)	1438 sh (m)	1447 sh (m)		1445 (m)	
ν_2	1685	1669 (w)	1671 (w)	not obs.	1660 (w)	1690 (w)	not obs.
$2\nu_4$		2878 (m)	2842 (m)	2852 (w)	2825 (w)	2844 (w)	2825 (m)
$\nu_2+\nu_4$		3043 (m)	2967 sh (m)	3091 sh (m)	3042 (m)	3065 (m)	3035 (m)
		3025 (m)					
$2\nu_2$		3140 (s)	3140 (s)	3179 sh (m)	3170 (w)	3187 sh (w)	3175 (m)
ν_3	3134	3223 (m)	3320 (m)	3233 sh (m)	3246 sh (m)	3288 (s)	3300 (s)
		3281 sh (w)		3294 (s)	3311 (s)		3455 sh (w)
		3333 sh (w)					

* Values for the free NH_4^+ molecule from Herzberg (1966).
† Values from Harlov et al. (2001b).
Abbreviations: as in Table 1; Budd: buddingtonite, Tob: tobelite, sh: shoulder, w: weak, m: medium, s: strong. For further explanation see text.

in Figure 4, along with the spectra of synthetic buddingtonite and tobelite (sample 13-99 from Pöter et al. (2007)). The free ammonium ion NH_4^+ has T_d symmetry resulting in four normal vibrational modes (Herzberg 1966): symmetric (ν_1) and antisymmetric (ν_3) stretching vibrations, and symmetric (ν_2) and antisymmetric (ν_4) bending vibrations (Kearley and Oxton 1983). All fundamentals are Raman-active, but only the triply degenerated states ν_3 and ν_4 are IR-active. However, in complex structures the NH_4 symmetry is reduced by the crystal field, so that the ν_1 and ν_2 bands appear in IR spectra, and the degeneracy of the ν_2, ν_3 and ν_4 bands may be annihilated to some extent. Positions of the NH_4 vibration modes in Figure 4 follow the assignments for buddingtonite (Harlov et al. 2001a). Table 4 summarizes band positions and relative intensities along with the fundamental frequencies of the free ammonium molecule (Nakamoto, 1986, after Landolt-Börnstein, 1951), but several studies (Likhacheva et al. 2002; Mookherjee et al. 2002a, b; Harlov et al. 2001b, c) show that in varying minerals the frequencies differ due to the crystal field and are mostly higher than the reported data for the free ion.

Ammonium incorporation into all new high-pressure phases is clearly demonstrated by the appearance of the NH_4 bending mode(s) ν_4, occurring in the range from 1397 to 1459 cm^{-1} (Fig. 4). Stretching mode(s) ν_3 appear at 3223 to 3333 cm^{-1} for NH_4-cymrite and NH_4-phengite (see also Harlov et al. 2001b, for NH_4-muscovite). There are no significant ν_3 modes for NH_4-hollandite and NH_4-Si-wadeite at these wavenumbers, instead, a strong band is present at about 3130 cm^{-1} for these two phases. One may speculate that this represents ν_3 due to a shift towards lower wavenumbers in the higher coordinated structures. A comparison between NH_4-phengite and tobelite show a wide accordance among the spectra, the small observable differences are caused by the additional Mg in the octahedral site of the phengite.

Due to the distortion of the crystal field, ν_2 appears as an additional weak band in the range from 1660 to 1690 cm^{-1}; further weak bands and shoulders arise from overtone and

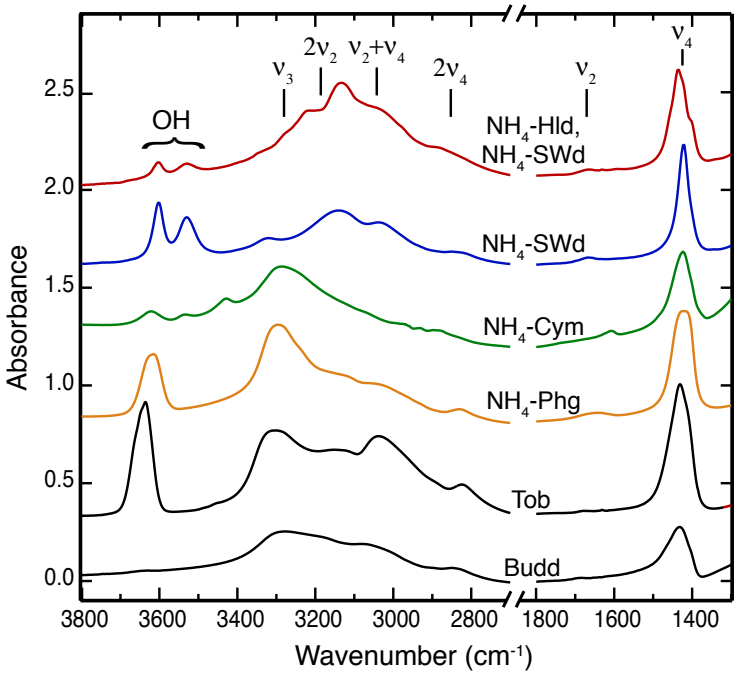

Figure 4: Mid-Infrared spectra of the run products of AW14-07 [NH_4-hollandite (31 wt%) plus NH_4-Si-wadeite (17 wt%)], AW28-07 (NH_4-Si-wadeite), AW22-07 (NH_4-cymrite), AW17-07 (NH_4-phengite), tobelite [see Pöter et al. (2007), their sample 13-99] and buddingtonite in the range from 1300 to 1800 and from 2700 to 3800 cm^{-1}. Spectra are shifted vertically. Relative proportions of NH_4-Hld and NH_4-SWd are calculated from Rietveld refinements. The normal modes on the basis of T_d symmetry for the NH_4-tetrahedron are marked as described by Harlov et al. (2001a) for buddingtonite. Additional OH-vibrations in the upper two spectra stem from OH-topaz (Table 1).

combination modes (Fig. 4, Table 4). A detailed description of the effective symmetry of the NH_4 molecule is not possible from IR spectra alone because ν_3, overtones $2\nu_2$ and $2\nu_4$, and combination modes $\nu_2 + \nu_4$ interfere with each other at similar wavenumbers (Harlov et al. 2001b). Therefore, the band assignments (Table 4), which are based on identified bands for buddingtonite and other NH_4-bearing minerals (Harlov 2001a, b, c; Pöter et al. 2007) represent only one of several possibilities.

Bands at 3531 and 3603 cm^{-1} as occurring in the spectra of the NH_4-hollandite and NH_4-Si-wadeite-bearing samples represent the two OH-stretching bands of OH-topaz (Wunder et al. 1993). NH_4-cymrite contains molecular water, consequently, in the NH_4-cymrite-bearing sample a H_2O bending mode at 1606 cm^{-1} and the OH-stretching modes at 3533 and 3621 cm^{-1} are present, the positions are the same as observed by Fasshauer et al. (1997) for K-cymrite. According to that study the shoulder, which can be observed at 3433 cm^{-1}, is also due to H_2O. The spectrum of NH_4-phengite shows the typical OH-stretching vibration of micas from 3604 to 3629 cm^{-1} (e.g., Harlov 2001b; Pöter et al. 2007).

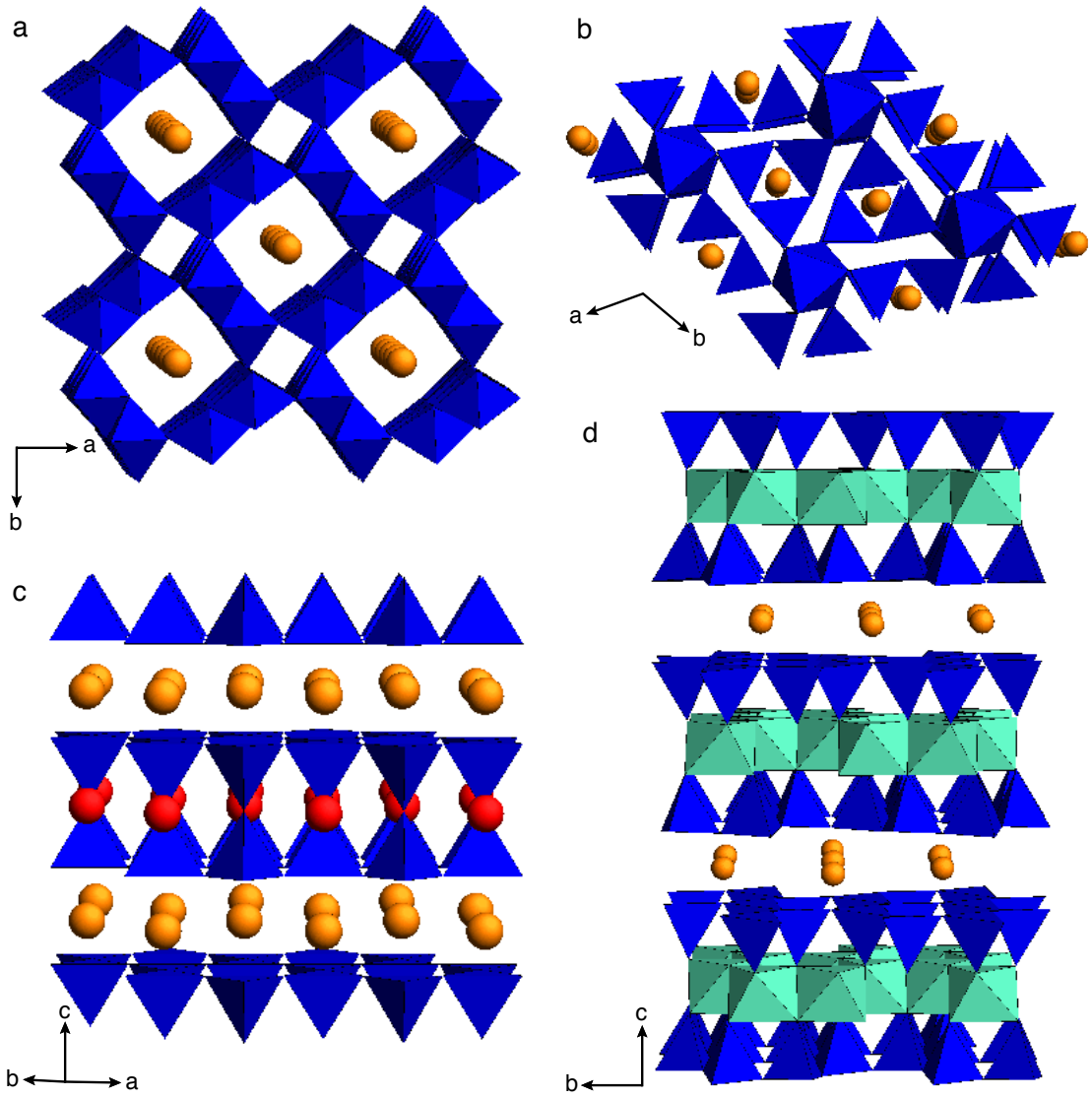

Figure 5: Projection of crystal structures of **(a)** NH_4-hollandite and **(b)** NH_4-Si-wadeite viewed down the c axis, **(c)** NH_4-cymrite; and **(d)** NH_4-phengite ($2M_1$ polytype) viewed along the a axis. The NH_4^+ ion is illustrated as sphere in orange, a possible ordering/disordering of the NH_4^+ cations in the crystal structures is neglected, as there was no hint from the XRD refinements. Si-containing tetrahedra and octahedra are shown in blue. The red balls in the NH_4-cymrite structure represent the H_2O-molecules. The light green octahedra in the phengite structure are occupied by Al and Mg.

Discussion

Crystal structure comparison between NH_4- and K-bearing phases

NH_4-hollandite [$NH_4AlSi_3O_8$]. The crystal structure of hollandite (Fig. 5a) is con-

structed of edge-sharing octahedra that form a four-sided eight-membered channel. The octahedra are randomly occupied to 3/4 with Si and 1/4 with Al. The channel is capable of incorporating low-valence large-radius cations in twelve-fold coordination, such as Na^+ (Liu et al. 1978), K^+ (Ringwood et al. 1967), and NH_4^+ (this study). The space group is $I4/m$. Comparison with K-hollandite reveals that the c lattice parameter remains largely unchanged whereas the a lattice parameter increases from 9.315 Å (K-hollandite; Zhang et al. 1993) to 9.423 Å (NH_4-hollandite; Table 2). The larger NH_4^+ ion significantly expands the diameter of the octahedra channels, but not the channel length. The cell volume increases from 236.3 $Å^3$ (K-hollandite) to 241.93 $Å^3$ (NH_4-hollandite). The same behavior can be observed in case of the smaller Na^+-ion. The a lattice parameter of Na-hollandite (9.30 Å) shows a significant reduction compared to K-hollandite, while the channel length remains nearly unchanged (c = 2.73 Å; Liu et al. 1978).

NH_4-Si-wadeite [$(NH_4)_2Si_4O_9$]. The crystal structure of NH_4-Si-wadeite and its K-analogue Si-wadeite [$K_2Si_4O_9$] (Kinomura et al. 1975; Yagi et al. 1994) is a framework structure consisting of parallel Si_3O_9-layers in an ABAB... stacking sequence along the c axis (Fig. 5b). The layers are linked by Si-occupied octahedra. In Si-wadeite 1/4 of the total Si is octahedrally coordinated and 3/4 is tetrahedrally coordinated. K^+ and NH_4^+ are nine-fold coordinated and sit in large cages, which occur between the A and B layers of the Si_3O_9 rings. The space group is $P6_3/m$. Comparison with K-Si-wadeite shows nearly identical c lattice parameters (Table 2), whereas the a lattice parameter increases from 6.6124 Å (K-Si-wadeite; Swanson and Prewitt 1983) to 6.726 Å (NH_4-Si-wadeite). Incorporation of NH_4 instead of K expands the diameter of the Si_3O_9-rings and hence the cages. Neither the stacking sequence of the layers nor their distance is changed. The cell volume increases from 360.1 (K-Si-wadeite) to 372.1 $Å^3$ (NH_4-Si-wadeite).

NH_4-cymrite [$NH_4AlSi_3O_8 \cdot H_2O$]. NH_4-cymrite and K-cymrite display a sheet-like crystal structure (Fig. 5c). Si and Al are randomly distributed on symmetrically equivalent tetrahedrally coordinated sites. The tetrahedra form hexagonal rings, which are further connected to double-layers via common opposite vertices. NH_4 and K in twelve-fold coordination are situated in the middle of the rings between two of these double-layers. Molecular water is located within the double six-membered tetrahedral rings, whereas its orientation along the c axis is yet unknown. The space group is $P6/mmm$. Compared to K-cymrite (c = 7.7057 Å; Fasshauer et al. 1997), NH_4-cymrite (c = 7.835 Å) shows the major increase in the c lattice parameter, whereas the a lattice parameter increases only by 0.5% (Table 2). This is typical for sheet-like structures, where substitution of larger monovalent interlayer cations for smaller ones drastically enlarges the distance between the sheets, whereas the six-membered tetrahedral rings are only slightly expanded. It has been argued that there is only one crystallographic site for molecular water in K-cymrite, due to the occurrence of only two peaks in the OH-stretching region (Thompson et al. 1998). The IR spectrum of NH_4-cymrite shows the same two peaks at the respective wavenumbers, so that no variation in the order of the water molecules is indicated.

NH_4-phengite [$NH_4(Mg_{0.5}Al_{1.5})(Al_{0.5}Si_{3.5})O_{10}(OH)_2$]. Comparison of the lattice parameters of $2M_1$ NH_4-phengite (Fig. 5d) with that of $2M_1$ K-phengite having nearly identical celadonite component (Massonne and Schreyer 1986) reveals that the c lattice parameter and angle β are significantly enlarged (19.972 Å vs 20.44 Å; 95.44° vs 95.71°) whereas the a and b lattice parameters show only a very slight increase (Table 2). In case

of the $1M$ polytypes the c lattice parameter is likewise increased but the angle β contracts by about 0.1%. There is a much larger difference in the a lattice parameters for the $1M$ polytypes compared to that for the $2M_1$ polytypes. This holds also for b, though to a minor extent. Similar variations in cell parameters between $1M$ and $2M_1$ polytypes of muscovite and tobelite, i.e., NH_4-muscovite, are documented in Pöter et al. (2007). The tetrahedral distortion due to tetrahedral rotation in dioctahedral micas is described by the rotation angle α, where $\cos\alpha = b/(9.051 + 0.254N)$ (Radoslovich and Norrish 1962; Bailey 1984). N is the number of tetrahedral Al atoms pfu and b is the lattice parameter. The tetrahedral rotation angle of $2M_1$ K-phengite with the celadonite component given above is calculated to 9.9°, that of $2M_1$ NH_4-phengite to 9.5° (Massonne and Schreyer 1986; Table 4). The larger NH_4^+ ion stretches not only the distance between the sheets but also reduces the extent of tetrahedral rotation in the NH_4- relative to the K-phengite. Differences may also exist in the development of the respective polytypes. Schmidt et al. (2001) synthesized K-phengites in the KMASH system at similar conditions and report that there is no clear dependence of the polytype distributions on their celadonite component, however, in the K-bearing system the $1M$ is much more abundant than the $3T$-polytype. This is quite the contrary to our NH_4-pengites ($3T$: 13.6 wt%; $1M$: 1 wt%) indicating that the larger NH_4^+ ion might favor formation of the $3T$-polytype.

Stabilities compared to K-analogues

The stability of NH_4-phases depends on the redox conditions. Conditions must be reducing to allow the formation of NH_3/NH_4^+ in the mineral-fluid system and to prevent oxidation to N_2. There is little information on the speciation of H–N–O fluids at very high pressures. Calculations using the perturbation theory-based equation of state of Churakov and Gottschalk (2003b) reveal that H–N–O fluids buffered by QFM in the relevant P–T range will consist almost exclusively of H_2O and N_2 (see also Simakov 1998; 2006). An abrupt transition is indicated at f_{O_2} between -2 and -3 log units below QFM so that towards more reducing conditions NH_3 and H_2O become the main species. Data on the dissociation constant $log(K)$ of $(NH_3)H_2O \leftrightarrow NH_4^+ + OH^-$ only exist for very dilute solutions up to 700 °C and 400 MPa (Quist and Marshall 1968). $Log(K)$ ranges from about 10–9 at fluid densities of 0.5 g/cm^3 to about 10–3 at 1.15 g/cm^3. Fluid densities in our experiments are much higher, up to 1.5–1.6 g/cm^3 (Churakov and Gottschalk 2003a, 2003b), and one may expect much stronger dissociation, the extent of which remains unknown. In any case, redox conditions in our experiments were sufficiently reducing to enable the formation of NH_4-silicates in presence of NH_3-bearing fluid, albeit some oxidation and formation of N_2 due to hydrogen loss may have occurred during the course of the experiments.

In the NASH system, the stabilities of high-pressure NH_4-silicates in the presence of fluid in P–T space broadly correspond to their K-analogues. K-cymrite is stable from 2.5 GPa, 400 °C to about 9 GPa, 1200 °C (Fasshauer et al. 1997; Thompson et al. 1998; Harlow and Davies 2004). The two experiments at 7.8 GPa, 800 °C on buddingtonite bulk composition are well located within the stability field of K-cymrite and produced NH_4-cymrite plus some coesite and kyanite as additional phases. Run AW22-07 was performed on nominally dry buddingtonite, without adding fluid. Even the breakdown of nominally dry buddingtonite along with a little amount of absorbed surface water, which could not be

avoided in sample preparation, provided sufficient NH_3- and H_2O-bearing fluid to stabilize NH_4-cymrite along with coesite and kyanite. At the given conditions and in presence of pure H_2O-fluid ($a_{H_2O} = 1$) OH-topaz is stable (Wunder et al. 1993); we, however, observe kyanite + H_2O. A possible interpretation is that due to the significant amounts of nitrogen-bearing species in the fluid the water activity is reduced, thus expanding the stability field of kyanite relative to OH-topaz. Towards higher pressure of 10 GPa at 700 °C, NH_4-Si-wadeite is formed, along with stishovite and OH-topaz, the latter stably replacing kyanite + H_2O (Wunder et al. 1993). This is similar to the K-bearing system, where K-Si-wadeite + kyanite + silica replaces K-cymrite as pressure increases (Davies and Harlow 2002). K-Si-wadeite + kyanite + stishovite produce K-hollandite at pressures higher than 8 to 9 GPa by a water-absent univariant reaction (Yong et al. 2008; Fig. 1). In the NH_4-bearing system, NH_4-Si-wadeite (+ OH-topaz + stishovite) persists at least up to 10 GPa. NH_4-hollandite appears at 12.5 GPa, 700 °C, together with NH_4-Si-wadeite, OH-topaz, kyanite, and stishovite. Taking the NH_4-bearing system as an analogue to the K-bearing system, it appears that both the low-pressure assemblage (NH_4-SWd + OH-Top/Ky + Stv) and the high-pressure phase (NH_4-Hld) were concurrently formed. This may indicate that our experimental conditions happened to meet the NH_4-hollandite-forming reaction curve and that the NH_4-hollandite-in reaction occurs at pressures a few GPa higher than that for K-hollandite. On the other hand, the reaction is not univariant because of shifts in the fluid composition due to hydrogen loss, and it may well be that the produced assemblage is transitional in response to changing activities of fluid phase components. The latter is somewhat supported by the presence of both kyanite and OH-topaz, probably resulting from changing water activity during the course of the experiment. In any case, stability relations of the high-pressure NH_4-silicates closely resemble that of their K-analogues in that the same sequence of K- and NH_4-cymrite, K- and NH_4-Si-wadeite, and K- and NH_4-hollandite occurs from lower to higher pressures along approximately the same pressure range.

In fluid-saturated metabasaltic and metapelitic model systems it has been experimentally shown that K-phengite is stable up to about 9.5 GPa, 750 to 1000 °C. At higher pressures, it breaks down to K-hollandite + clinopyroxene-bearing assemblages (Domanik and Holloway 1996; Schmidt 1996; Schmidt and Poli 1998; Poli and Schmidt 2002). Clinopyroxene formed at these conditions incorporates about 1 wt% of K_2O (Schmidt and Poli 1998; Bindi et al. 2006). We synthesized NH_4-phengite at 4 GPa, 700 °C. There is again no information on its upper pressure stability, however, given the strong similarities between the KASH and NASH systems one may reasonably assume that NH_4-phengite in natural systems would react to NH_4-hollandite + clinopyroxene-bearing assemblages at similar pressure. If so, incorporation of significant amounts of NH_4 into high-pressure clinopyroxene is possible. As K-hollandite may persist up to 95 GPa, 2300 °C (cf. above) it is conceivable that NH_4-hollandite is also stable at conditions through the transition zone to the lower mantle.

Implications for nitrogen and hydrogen transport into Earth's mantle

At conditions of 500 to 600 °C, 0.2 to 0.4 GPa the binaries K-muscovite–NH_4-muscovite (tobelite), K-feldspar–NH_4-feldspar (buddingtonite), and K-phlogopite–NH_4-phlogopite form complete solid solution series (Bos et al. 1988; Pöter et al. 2004, 2007). Given the similarities in structure and stability relations, this probably holds also for the high-pressure

end-members. In any case, high-pressure K-phases are expected to be able to incorporate large amounts of NH_4 into their structures. If so, NH_4 can be continuously redistributed into solids when high-pressure K-phases are successively generated at conditions of subducting slabs. This provides an important means for nitrogen transport into the deep mantle (see also Busigny et al. 2003; Thomassot et al. 2007).

Incorporation of ammonium into K-hollandite and possibly high-pressure clinopyroxene and transport into the deeper mantle may have another important implication. There is a wealth of experimental work addressing the actual concentrations and the storage capacity of H_2O in nominally anhydrous minerals in the upper mantle down to the transition zone (for summaries see Hirschmann et al. 2005; Keppler and Bolfan-Casanova 2006). There is overall agreement that the H_2O storage capacity in nominally anhydrous mantle assemblages just above the transition zone amounts to about 0.4 wt% (Hirschmann et al. 2005) and to at least 5 times higher when wadsleyite becomes stable. Bromiley and Keppler (2004) argued that omphacitic clinopyroxene is the main OH-bearing phase in subducted eclogites after breakdown of hydrous minerals with maximum concentrations of a few hundred wt-ppm of H_2O, dependent on clinopyroxene composition and pressure. Natural omphacites usually have several hundred with maximum concentrations of about 1000 wt-ppm H_2O (Skogby 2006). It would thus appear that omphacites and their breakdown products were unable to feed the transition zone with large amounts of water. If, on the other hand, most of the available NH_4 in eclogite-facies rocks can be stored in K-rich phases such as clinopyroxene and hollandite to greater depth, this would provide a formidable mechanism of hydrogen transport into the transition zone and beyond. If so, the fate of any possible NH_4-silicate component at depths of the transition zone would be subject to the redox conditions, of which no sound information is currently available. Hypothetical oxidation reactions of the type NH_4-component in solid + O_2 → solid(s) + N_2 + H_2O would produce water and molecular nitrogen, forming two H_2O molecules from one NH_4; under reducing conditions NH_4 component in solids would form ammonia and water by reaction to solid(s) + NH_3 + H_2O; and one may even speculate that under very reducing conditions nitrides or oxonitride component in oxides and hydrogen could possibly be generated. The latter is certainly speculative, however, if one accepts that highly reduced phases such as moissanite and Fe-silicides included in deep-seated diamonds (e.g., Moore et al. 1986; Otter and Gurney 1989; Leung et al. 1990, 1996) or in kimberlitic rocks (Mathez et al. 1995; Di Pierro et al. 2003) represent redox conditions of certain, albeit limited regions of the mantle, oxygen fugacities of 5 to 6 log units below the iron-wuestite buffer were indicated (e.g., Mathez et al. 1995). At about that conditions nitrides or oxonitrides may also become stable, and it may well be that they provide another solid sink for nitrogen in the deep Earth, aside from nitrogen in diamonds.

Sediments and metasediments may contain several thousands of wt-ppm of ammonium present in clay minerals, micas and feldspars, which is continuously redistributed into newly formed high-pressure K-bearing phases along rocks' P–T path during subduction. This provides the means for nitrogen and hydrogen transport down to the transition zone of the Earth's mantle and possibly to even greater depth. Ammonium as a component is potentially very important for long-time, large-scale recycling of hydrogen and nitrogen between the Earth's surface and the deep mantle.

Acknowlegdements

We thank A. Hahn and R. Schulz for technical assistance, U. Gernert (ZELMI, Technical University of Berlin) for providing SEM facilities, D. Rhede and O. Appelt for help with EMP work, and M. Gottschalk for fruitful discussions. The reviews by M. Mookherjee and J. Konzett, and the editorial comments by E. Libowitzky helped to improve the manuscript and were highly appreciated. This work was supported by the German Science Foundation [He 2015/(8-1)] within the framework of the Priority Program 1236 "Structures and properties of crystals at extreme pressures and temperatures" which is gratefully acknowledged.

References

Akaogi, M., Yusa, H., Shiraishi, K., and Suzuki, T. (1995) Thermodynamic properties of α-quartz, coesite, and stishovite and equilibrium phase relations at high pressures and high temperatures. Journal of Geophysical Research, 100, 22337-22347.

Bailey, S.W. (1984) Crystal chemistry of the true micas. In S.W. Bailey, Eds., Micas, 13, p. 13-60. Reviews in Mineralogy, Mineralogical Society of America, Chantilly, Virginia.

Bebout, G.E. and Fogel, M.L. (1992) Nitrogen-isotope compositions of metasedimentary rocks in the Catalina schists, California: Implications for metamorphic devolatilization history. Geochimica et Cosmochimica Acta, 56, 2839-2849.

Bebout, G.E., Cooper, D.C., Bradley, A.D., and Sadofsky, S.J. (1999) Nitrogen-isotope record of fluid-rock interactions in the Skiddaw aureole and granite, English Lake District. American Mineralogist, 84, 1495-1505.

Bindi, L., Downs, R.T., Harlow, G.E., Safonov, O.G., Litvin, Y.A., Perchuk, L.L., Uchida, H., and Menchetti, S. (2006) Compressibility of synthetic potassium-rich clinopyroxene: In-situ high-pressure single-crystal X-ray study. American Mineralogist, 91, 802-808.

Bos, A., Duit, W., Van der Eerden, A.M.J., and Jansen J.B.H. (1988) Nitrogen storage in biotite: an experimental study of ammonium and potassium partitioning between 1M-phlogopite and vapor at 2 kb. Geochimica et Cosmochimica Acta, 52, 1275-1283.

Bromiley, G.D. and Keppler, H. (2004) An experimental investigation of hydroxyl solubility in jadeite and Na-rich clinopyroxenes. Contributions to Mineralogy and Petrology, 147, 189-200.

Busigny, V., Cartigny, P., Philippot, P. Ader, M., and Javoy, M. (2003) Massive recycling of nitrogen and other fluid-mobile elements (K, Rb, Cs, H) in a cold slab environment: evidence from HP to UHP oceanic metasediments of the Schistes Lustrés nappe (western Alps, Europe). Earth and Planetary Science Letters, 215, 27-42.

Cartigny, P. and Ader, M. (2003) A comment on "The nitrogen record of crust-mantle interaction and mantle convection from Archean to Present" by B. Marty and N. Dauphas. Earth and Planetary Science Letters, 206, 397-410.

Churakov, S.V. and Gottschalk, M. (2003a) Perturbation theory based equation of state for polar molecular fluids: I. Pure fluids. Geochimica et Cosmochimica Acta, 67, 2397-2414.

Churakov, S.V. and Gottschalk, M. (2003b) Perturbation theory based equation of state for polar molecular fluids: II. Fluid mixtures. Geochimica et Cosmochimica Acta, 67, 2415-2425.

Davies , R.M. and Harlow, G.E. (2002) The high pressure stability of K-cymrite and phases in the system $Or - H_2O$. American Geophysical Union, Fall Meeting 2002, Abstract No.V72B-1308.

Di Pierro, S., Gnos, E., Grobety, B.H., Armbruster, T., Bernasconi, S.M., and Ulmer, P. (2003) Rock-forming moissanite (natural α-silicon carbide). American Mineralogist, 88, 1817-1821.

Domanik, K.J. and Holloway, J.R. (1996) The stability and composition of phengitic muscovite and associated phases from 5.5 to 11 GPa: implications for deeply subducted sediments. Geochimica et Cosmochimica Acta, 60, 4133-4154.

Fasshauer, D.W., Chatterjee, N.D., and Marler, B. (1997) Synthesis, structure, thermodynamic properties, and stability relations of K-cymrite, $K[AlSi_3O_8] \cdot H_2O$. Physics and Chemistry of Minerals, 24, 455-462.

Fischer, T.P., Hilton, D.R., Zimmer, M.M., Shaw, A.M., Sharp, Z.D., and Walker, J.A. (2002) Subduction and recycling of nitrogen along the Central American Margin. Science, 297, 1154-1157.

Fischer, T.P., Takahara, N., Sano, Y., Sumino, H., and Hilton, D.R. (2005) Nitrogen isotopes in the mantle: Insights from mineral separates. Geophysical Research Letters, 32, L11305.

Griffiths, P.R. and de Haseth, J.A. (1986) Fourier transform infrared spectroscopy. John Wiley and Sons, New York.

Harlov, D.E., Andrut, M., and Pöter, B. (2001a) Characterisation of buddingtonite $(NH_4)[AlSi_3O_8]$ and ND_4-buddingtonite $(ND_4)[AlSi_3O_8]$ using IR spectroscopy and Rietveld refinement of XRD spectra. Physics and Chemistry of Minerals, 28, 188-198.

Harlov D.E., Andrut, M., and Pöter, B. (2001b) Characterisation of tobelite $(NH_4)Al_2[AlSi_3O_{10}](OH)_2$ and ND_4-tobelite $(ND_4)Al_2[AlSi_3O_{10}](OD)_2$ using IR spectroscopy and Rietveld refinement of XRD spectra. Physics and Chemistry of Minerals, 28, 268-276.

Harlov, D.E., Andrut, M., and Melzer S (2001c) Characterisation of NH_4-phlogopite $(NH_4)[Mg_3AlSi_3O_{10}](OH)_2$ and ND_4-phlogopite $(ND_4)[Mg_3AlSi_3O_{10}](OD)_2$ using IR spectroscopy and Rietveld refinement of XRD spectra. Physics and Chemistry of Minerals, 28, 77-86.

Harlow, G.E. and Davies R.M. (2004) Status report on stability of K-rich phases at mantle conditions. Lithos, 77, 647-653.

Herzberg, G. (1966) Molecular Spectra and Molecular Structure Vol.2: Infrared and Raman Spectra of Polyatomic Molecules. Van Nostrand, Princeton.

Hirschmann, M.M., Aubaud, C., and Withers, A. (2005) Storage capacity of H_2O in nominally anhydrous minerals in the upper mantle. Earth and Planetary Science Letters, 236, 167-181.

Javoy, M., Pineau, F., and Delorme, H. (1986) Carbon and nitrogen isotopes in the mantle. Chemical Geology, 57, 41-62.

Kearley, G.J. and Oxton, L.A. (1983) Recent advances in the vibrational spectroscopy of ammonium ion in crystal. In R.J.H. Clark et R.E. Hesters, Eds., Advances in Infrared and Raman Spectroscopy, 10, Chap. 2, John Wiley and Sons, New York.

Keppler, H. and Bolfan-Casanova, N. (2006) Thermodynamics of water solubility and partitioning. In H. Keppler and J.R. Smyth, Eds., Water in nominally anhydrous minerals, 62, p. 193-230. Reviews in Mineralogy and Geochemistry, Mineralogical Society of America and Geochemical Society, Chantilly, Virginia.

Kinomura, N., Kume, S., and Koizumi, M. (1975) Synthesis of $K_2SiSi_3O_9$ with silicon in 4- and 6-coordination. Mineralogical Magazine, 40, 401-404.

Konzett, J. and Fei, Y. (2000) Transport and storage of potassium in the Earth's upper mantle and transition zone: an experimental study to 23 GPa in simplified and natural bulk compositions. Journal of Petrology, 41, 583-603.

Landolt-Börnstein (1951) Physikalisch-chemische Tabellen, Vol. 2, Springer, Berlin.

Larson, A.C. and von Dreele, R.B. (2004) Generalized structure analysis system. Alamos National Laboratory Report LAUR 96-748. Los Alamos National Laboratory, New Mexico.

Leung, I.S., Guo, W., Freidman, I., and Gleanson, J. (1990) Natural occurrence of silicon carbide in a diamondiferous kimberlite from Fuxian. Nature, 346, 352-354.

Leung, I.S., Taylor, L.A., Tsao, C.S., and Han, Z. (1996) SiC in diamond and kimberlites: Implications for nucleation and growth of diamond. International Geology Review, 38, 595-606.

Likhacheva, A.Yu., Paukshtis, E.A., Seryotkin, Yu.V. and Shulgenko, S.G. (2002) IR spectroscopic characterization of NH_4-analcime. Physics and Chemistry of Minerals, 29, 617-623.

Liu, L.G. (1978) High-pressure phase transformations of albite, jadeite and nepheline. Earth and Planetary Science Letters, 37, 438-444.

Marty, B. (1995) Nitrogen content of the mantle inferred from $N_2 - Ar$ correlation in oceanic basalts. Nature, 377, 326-329.

Marty, B. and Dauphas, N. (2003a) The nitrogen record of crust-mantle interaction and mantle convection from Archean to Present. Earth and Planetary Science Letters, 206, 397-410.

Marty, B. and Dauphas, N. (2003b) Nitrogen isotopic composition of the present mantle and the Archean biosphere: Reply to comment by Pierre Cartigny and Magali Ader. Earth and Planetary Science Letters, 216, 433-439.

Massonne, H-J. and Scheyer W. (1986) High-pressure syntheses and X-ray properties of white micas in the system $K_2O - MgO - Al_2O_3 - H_2O$. Neues Jahrbuch Mineralogische Abhandlungen, 153, 177-215.

Mather, T.A., Allen, A.G., Bavison, B.M., Pyle, D.M., Oppenheimer, C., and McGonigle, A.J.S. (2004) Nitric acid from volcanoes. Earth and Planetary Science Letters, 218, 17-30.

Mathez, E.A., Fogel, R.A., Hutcheon, I.D., and Marshintsev, V.K. (1995) Carbon isotopic composition and origin of SiC from kimberlites of Yakutia, Russia. Geochimica et Cosmochimica Acta, 59, 781-791.

Melzer, S. and Wunder, B. (2000) Island-arc basalt alkali ratios: constraints from phengite-fluid partitioning experiments. Geology, 28, 583-586.

Mertz, L. (1965) Transformation in Optics. Wiley, New York.

Mingram, B. and Bräuer, K. (2001) Ammonium concentration and nitrogen isotope composition in metasedimentary rocks from different tectonometamorphic units of the European Variscan Belt. Geochimica et Cosmochimica Acta, 65, 273-287

Mohapatra, R.H. and Murty, S.V.S. (2000) Search for the mantle nitrogen in the ultramafic xenoliths from San Carlos, Arizona. Chemical Geology, 164, 305-320.

Mookherjee, M., Redfern S.A.T., Zhang, M., and Harlov, D.E. (2002a) Orientational order-disorder in synthetic ND_4/NH_4-phlogopite: a low-temperature infrared study. European Journal of Mineralogy, 14, 1033-1039.

Mookherjee, M., Redfern S.A.T., Zhang, M., and Harlov, D.E. (2002b) Orientational order-disorder of $N(D,H)_4^+$ in tobelite. American Mineralogist, 87, 1686-1691.

Moore, R.O., Otter, M.L., Rickard, R.S., Harris, J.W, and Gurney, J.J. (1986) The occurrence of moissanite and ferri-periclase as inclusions in diamond. In 4^{th} International Kimberlite Conference, Perth, Extended Abstracts; Abstract Geological Society of Australia, 16, 409-411.

Nakamoto, K. (1986) Infrared and Raman spectra of inorganic and co-ordination compounds. Wiley, New York.

Nishihara, Y., Matsukage, K.N., and Karato, S.-I. (2006) Effects of metal protection coils on thermocouple EMF in multi-anvil high-pressure experiments. American Mineralogist, 91, 111-114.

Otter, M.L. and Gurney, J.J. (1989) Mineral inclusions in diamonds from the Sloan diatreme, Colorado-Wyoming State Line Kimberlite District, North America. In Kimberlite and Related Rocks, Volume 2, Their Mantle/Crust Setting, Diamonds and Diamond Exploration; Geological Society of Australia, Special Publication, 14, p. 1042-1053, Blackwell Scientific, Cambridge, UK.

Pinti, D.L., Hashizume, K., and Matsuda, J.I. (2001) Nitrogen and argon signatures in 3.8 to 2.8 Ga metasediments: Clues on the chemical state of the Archean ocean and deep biosphere. Geochimica and Cosmochimica Acta, 65, 2301-2315.

Pitcairn, I.K., Teagle, D.A.H., Kerrich, R., Craw, D., and Brewer, T.S. (2005) The behaviour of nitrogen and nitrogen isotopes during metamorphism and mineralization: Evidence from the Otago and Alpine schists, New Zealand. Earth and Planetary Science Letters, 233, 229-246.

Poli, S. and Schmidt, M. (2002) Petrology of subducted slabs. Annual Review of Earth and Planetary Sciences, 207-235.

Pöter, B., Gottschalk, M., and Heinrich, W. (2004) Experimental determination of the K-NH_4-partitioning between muscovite, K-feldspar, and aqueous chloride solutions. Lithos, 74, 67-90.

Pöter, B., Gottschalk, M., and Heinrich, W. (2007) Crystal-chemistry of synthetic K-feldspar–buddingtonite and muscovite–tobelite solid solutions. American Mineralogist, 92, 151-165.

Quist, A.S, and Marshall W.L. (1968) Ionization equilibria in ammonia-water solutions to 700 °C and to 4000 bars of pressure. Journal of Physical Chemistry, 72, 3122-3128.

Radoslovich, E.W. and Norrish, K. (1962) The cell dimensions and symmetry of layer-lattice silicates. American Mineralogist, 47, 599-616.

Ringwood, A.E., Reid, A.F., and Wadsley, A.D. (1967) High-pressure $KAlSi_3O_8$, an aluminosilicate with sixfold coordination. Acta Crystallographica, 23, 1093-1095.

Sadofsky, S.J. and Bebout, G.E. (2000) Ammonium partitioning and nitrogen-isotope fractionation among coexisting micas during high-temperature fluid-rock interactions: Examples from the New England Appalachians. Geochimica et Cosmochimica Acta, 64, 2835-2849.

Sano, Y., Takahata, N., Nishio, Y., Fischer T.P., and Williams S.N. (2001) Volcanic flux of nitrogen from the Earth. Chemical Geology, 171, 263-271.

Schmidt, M.W. (1996) Experimental constraints on recycling of potassium from subducted oceanic crust. Science, 272, 1927-1930.

Schmidt, M. and Poli, S. (1998) Experimentally based water budgets for dehydrating slabs and consequences for arc magma generation. Earth and Planetary Science Letters, 163, 361-379.

Schmidt, M. and Ulmer, P. (2004) A rocking multianvil: elimination of chemical segregation in fluid-saturated high-pressure experiments. Geochimica et Cosmochimica Acta, 68, 1889-1899.

Schmidt, M.W., Dugnani, M., and Artioli, G. (2001) Synthesis and characterization of white micas in the join muscovite-aluminioceladonite. American Mineralogist, 86, 555-565.

Shannon, R.D. (1976) Revised effective ionic radii and systematic studies of interatomic distances in halides and chalcogenides. Acta Crystallographica, A32, 751-767.

Simakov, S.K. (1998) Redox state of upper mantle peridotites under the ancient cratons and its connection with diamond genesis. Geochimica et Cosmochimica Acta, 62, 1811-1820.

Simakov, S.K. (2006) Redox state of eclogites and peridotites from sub-cratonic upper mantle and a connection with diamond genesis. Contributions to Mineralogy and Petrology, 151, 282-296.

Skogby, H. (2006) Water in natural mantle minerals I: Pyroxenes. In H. Keppler and J.R. Smyth, Eds., Water in nominally anhydrous minerals, 62, p. 155-167. Reviews in Mineralogy and Geochemistry, Mineralogical Society of America and Geochemical Society, Chantilly, Virginia.

Swanson, D.K. and Prewitt, C.T. (1983) The crystal structure of $K_2Si^{VI}Si_3^{IV}O_9$. American Mineralogist, 68, 581-585.

Thomassot, E., Cartigny, P., Harris, J.P., and Viljoen K.S. (2007) Methane-related diamond crystallization in the Earth's mantle: Stable isotope evidences from a single diamond-bearing xenolith. Earth and Planetary Science Letters, 257, 362-371.

Thompson, P., Parsons, I. Graham, C.M., and Jackson, B. (1998) The breakdown of potassium feldspar at high water pressures. Contributions to Mineralogy and Petrology, 130, 176-186.

Truckenbrodt, J., Ziegenbein, D., and Johannes, W. (1997) The different behavior of boron nitride and unfired pyrophyllite assemblies. American Mineralogist, 82, 337-344.

Tutti, F., Dubrovinsky, L.S., Saxena S.K., and Carlson S. (2001) Stability of $KAlSi_3O_8$ hollandite-type structure in the Earth's lower mantle conditions. Geophysical Research Letters, 28, 14, 2735-2738.

Urakawa, S., Kondo, T., Igawa, N., Shimomura, O., and Ohno, H. (1994) Synchroton radiation study on the high-pressure and high-temperature phase relations of $KAlSi_3O_8$. Physics and Chemistry of Minerals, 21, 387-391.

Williams, L.B., Wilcoxon, B.R., Ferrell, R.E., and Sassen, R. (1992) Diagenesis of ammonium during hydrocarbon maturation and migration, Wilcox Group, Louisiana, USA. Applied Geochemistry, 7, 123-134.

Wunder, B. (1998) Equilibrium experiments in the system $MgO - SiO_2 - H_2O$ (MSH): stability fields of clinohumite-OH [$Mg_9Si_4O_{16}(OH)_2$], chondrodite-OH [$Mg_5Si_2O_8(OH)_2$] and phase A ($Mg_7Si_2O_8(OH)_6$). Contributions to Mineralogy and Petrology, 132, 111-120.

Wunder, B., Rubie, D.C., Ross II, C.R., Medenbach, O., Seifert, F., and Schreyer, W. (1993) Synthesis, stability, and properties of $Al_2SiO_4(OH)_2$: A fully hydrated analogue of topaz. American Mineralogist, 78, 285-297.

Yagi, A., Suzuki, T., and Akaogi. M. (1994) High pressure transition in the system $KAlSi_3O_8 - NaAlSi_3O_8$. Physics and Chemistry of Minerals, 21, 12-17.

Yong, W., Dachs, E., Withers, A.C., and Essene E.J. (2008) Heat capacity and phase equilibria of wadeite-type $K_2Si_4O_9$. Contributions to Mineralogy and Petrology, 155, 137-146.

Zhang, J., Ko, J., Hazen, R.M., and Prewitt, C.T. (1993) High-pressure crystal chemistry of $KAlSi_3O_8$ hollandite. American Mineralogist, 78, 493-499.